



HAL
open science

Modeling of an infrared stationary micro-spectrometer integrated on a focal plane array

S. Mouzali, S. Lefebvre, S. Rommeluère, Y. Ferrec, J. Primot

► **To cite this version:**

S. Mouzali, S. Lefebvre, S. Rommeluère, Y. Ferrec, J. Primot. Modeling of an infrared stationary micro-spectrometer integrated on a focal plane array. 6th International Symposium on Optronics - OPTRO 2014, Jan 2014, PARIS, France. hal-01059745

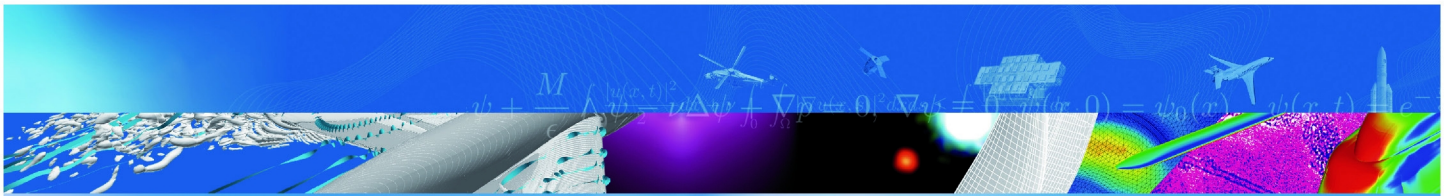
HAL Id: hal-01059745

<https://onera.hal.science/hal-01059745>

Submitted on 1 Sep 2014

HAL is a multi-disciplinary open access archive for the deposit and dissemination of scientific research documents, whether they are published or not. The documents may come from teaching and research institutions in France or abroad, or from public or private research centers.

L'archive ouverte pluridisciplinaire **HAL**, est destinée au dépôt et à la diffusion de documents scientifiques de niveau recherche, publiés ou non, émanant des établissements d'enseignement et de recherche français ou étrangers, des laboratoires publics ou privés.



T I R É À P A R T

**Modeling of an infrared
stationary
micro-spectrometer
integrated on a focal plane
array**

S. Mouzali, S. Lefebvre, S. Rommeluère,
Y. Ferrec, J. Primot

6th International Symposium on Optronics
OPTRO 2014
PARIS, FRANCE
28-30 janvier 2014

TP 2014-154

ONERA

THE FRENCH AEROSPACE LAB

r e t o u r s u r i n n o v a t i o n

Modeling of an infrared stationary micro-spectrometer integrated on a focal plane array

*Modélisation d'un micro-spectromètre infrarouge stationnaire intégré sur un plan focal
infrarouge*

par

S. Mouzali, S. Lefebvre, S. Rommeluère, Y. Ferrec, J. Primot

Résumé traduit :

Microspoc (MICRO spectromètre On Chip) est un concept de spectromètre infrarouge miniaturisé , avec un interféromètre statique à transformée de Fourier, intégrée sur une matrice de HgCdTe appelée Plan Focal Infrarouge (PFIR). La cavité de l'interféromètre est réalisée par amincissement du substrat, ce qui crée un interférogramme bidimensionnel à l'intérieur de la couche active du PFIR. Non seulement il est compact, mais ce spectromètre instantané fournit également une acquisition très rapide des signatures spectrales (jusqu'à quelques centaines de Hz), avec environ 155 bandes comprises entre 1,5 μm et 5 μm . Cependant, une simple inversion par transformée de Fourier des interférogrammes n'est pas suffisante pour obtenir une bonne qualité de spectres, en raison des interférences parasites à l'intérieur de la couche active du photodétecteur. Ainsi, un modèle a été établi pour une inversion plus robuste, décrivant la réponse de l'instrument à une scène. Il prend en compte le phénomène d'interférence , et diverses propriétés opto-géométriques du détecteur , comme les disparités de longueurs d'onde de coupure des pixels. L'approche de modélisation est présentée dans le présent document, et les premiers résultats prometteurs sont exposés .

MODELING OF AN INFRARED STATIONARY MICRO-SPECTROMETER INTEGRATED ON A FOCAL PLANE ARRAY

Salima Mouzali ⁽¹⁾, Sidonie Lefebvre ⁽¹⁾, Sylvain Rommeluère ⁽¹⁾, Yann Ferrec ⁽¹⁾, Jérôme Primot ⁽¹⁾

⁽¹⁾ ONERA – The French Aerospace Lab, Chemin de la Hunière, 91123 Palaiseau Cedex, France
salima.mouzali@onera.fr

KEYWORDS: IR cooled and uncooled, spectroscopic imagers, physical model, analytical model, simulation

ABSTRACT:

During the last few years, considerable efforts have been made in developing innovative spectrometric techniques at ONERA [1,2]. These instruments are dedicated to applications such as measurements of chemical agents spectral signatures, high temperature gas or objects at room temperature. There is therefore a real need for dedicated technology, as well as embedded processing modules able to extract the radiometric physical parameter from a raw signal. In this paper, a modeling approach for a static infrared spectrometer, Microspoc, is discussed in order to obtain good quality spectra.

1. MICROSPOC DESCRIPTION

1.1. The detector characteristics

Microspoc (MICRO SPectrometer On Chip) is a concept of miniaturized infrared cooled spectrometer [3,4]. It is based on a static Fourier transform interferometer integrated on a classical Mercury-Cadmium-Telluride Focal Plane Array (FPA), of 640 x 512 pixels.

The interferometer cavity is made by grinding the substrate to the shape of a wedge, with an angle of 6 mrad. Thus, a bi-dimensional interferogram is created inside the active layer of the FPA. Not only it is a compact instrument presenting the advantages of stationary Fourier spectrometers [5,6,7], but this snapshot spectrometer also provides very fast acquisition of spectral signatures (up to few hundreds of Hz), with about 155 bands between 1,5 μm and 5 μm .

The advantage of this type of device is, on the one hand, the high rates of acquisition available (up to 1 kHz), and, on the other hand, the measurements dynamics. As a matter of fact, the interferogram is directly projected on the detection plane,

simplifying the access to information on the spectra. Fig. 1 shows a schematic view of the detector.

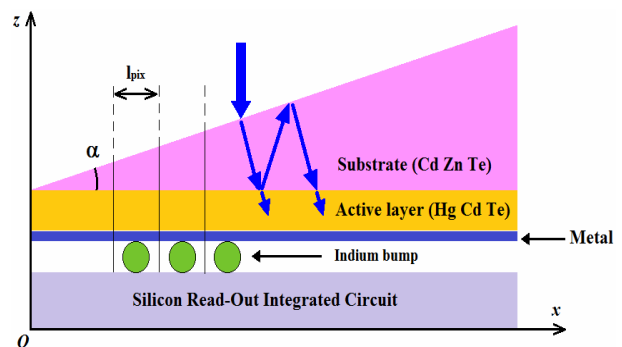


Figure 1. Diagram of Microspoc device

1.2. Spectral resolution

We define the spectral resolution under the assumption that the FPA delivers a two-dimensional interferogram made of linear fringes, representing a two-wave interference phenomenon. The optical path difference varies increasingly with the substrate thickness. The maximum optical path difference δ_{\max} determines the spectral resolution of the system $d\sigma$, as shown by Eq. 1 and Eq.2.

$$d\sigma = \frac{1}{2\delta_{\max}} \quad (1)$$

$$\delta_{\max} = 2n_s \cdot N_{pix} \cdot l_{pix} \cdot \tan \alpha \quad (2)$$

where α is the angle of the wedge, l_{pix} is the size of the pixels (15 μm in this case), N_{pix} is the number of operational pixels in the thinning direction of the device ($N_{pix} = 520$ among the 640 pixels available), and n_s is the optical refractive index of the substrate ($n_s = 2,72$).

Thus, for an angle equal to 6 mrad, the resolution obtained is about 19 cm^{-1} . It is possible to improve this value to 7 cm^{-1} , for instance, by increasing the angle α up to 15 mrad, which is technologically

achievable. However, one must remind that the main benefit of this device lies in the very fast acquisition of spectral signatures (up to 700 Hz), with a moderate spectral resolution.

1.3. Previous results

The quality of the first spectra obtained using Fourier transform inversion is limited by parasitic oscillations [8]. This is due to an inadequate consideration of the system characteristics.

Indeed, the use of thousands of individual detectors to generate a spectral information creates several problems, such as the fixed spatial noise, traducing the wavelength cutoff disparities of the pixels [9].

Thus, it is important to improve inversion methods in order to achieve more mature and valuable instruments, with high radiometric performance. A new inversion approach is proposed in this paper, based on the modeling of the absorption phenomenon inside the structure.

As previously mentioned, a two-wave interference phenomenon is considered at first approximation. As shown in Fig. 2, the experimental pixel efficiency matches a two-wave interference law only for a limited spectral range, corresponding to a wave number greater than 2400 cm^{-1} .

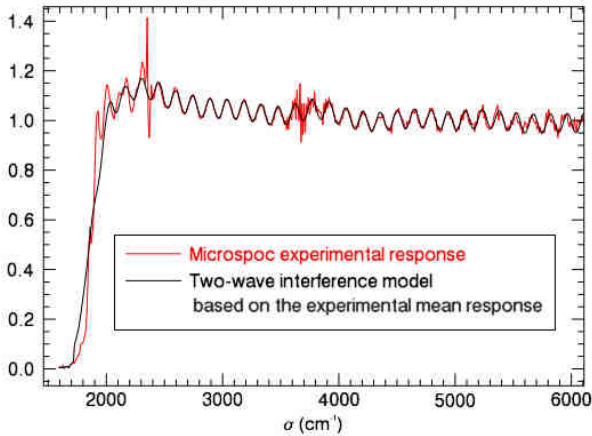


Figure 2. Superposition of normalized measured Microspoc detector response and a theoretical two-wave interference response

Actually, the active zone is not totally absorbent in the range of $[1600 \text{ cm}^{-1}, 2400 \text{ cm}^{-1}]$, which leads to the presence of several waves interfering into the entire structure, and not only into the substrate [8,10].

Hence, a Fourier transform description, based on two-wave interference is not sufficient to explain the interference phenomenon. We thereby developed two models of the instrument response,

accounting for several waves, in order to broaden the spectral range of the inversion.

2. MODELING APPROACH

2.1. Interferogram modeling

The interferogram I measured when observing a scene spectrum S can be described, assuming an additive noise, by Eq. 3,

$$I(x) = \left[M(\sigma, x) \right] \left[S(\sigma) \right] + n(x) \quad (3)$$

where σ is the wave number, $n(x)$ represents the experimental noise of the pixel x , $M(\sigma, x)$ is the matrix of the pixels spectral response in the FPA.

Consequently, the estimated spectrum S_{est} can be derived by Eq. 4,

$$S_{\text{est}}(x) = \left[M^\dagger(\sigma, x) \right] \left[I(x) \right] \quad (4)$$

where M^\dagger represents the generalized inverse of the matrix M , that can be obtained using singular value decomposition, for instance. The expression of the generalized inverse in this case is given by Eq. 5.

$$M^\dagger = (M^T M)^{-1} M^T \quad (5)$$

M could be measured by a test bench such as the one described in [11]. However, the uncertainties on the experimental setup limits the results precision. These uncertainties are mainly due to the relative poorness of illumination uniformity, the lack of knowledge of the internal source spectrum, and the atmospheric spectral transmission.

Consequently, we propose a modeling approach of the detector response in order to obtain an approximation of the matrix M , allowing to obtain good quality spectra. We developed two models: a physical one and an analytical one. These models do not take into account the substrate angle.

2.2. Multilayer model

The detector is modeled by a superposition of $N-1$ layers [12,13]. Each layer is supposed to be a homogeneous and isotropic dielectric medium.

As shown on Fig. 3, the z -axis is supposed to be in the direction of the normal to the planes limiting the

layer, which is supposed to be unbounded in the x - and y -directions. We consider here only the normal incidence (propagation in z -direction), as oblique incidence can easily be deduced from this case.

Each layer is characterized by the thickness d , the magnetic permeability μ , and the complex dielectric constant ϵ . These constants can be expressed by Eq. 6 and Eq. 7,

$$\mu = \mu_r \mu_0 \quad (6)$$

$$\epsilon = \epsilon_r \epsilon_0 \quad (7)$$

where μ_0 and ϵ_0 are respectively the vacuum permittivity and permeability. In practice, μ_r is unity, as the mediums considered are non-magnetic. Besides, we consider Eq. 8,

$$\epsilon_r \approx n^2 = (\eta - i\kappa)^2 \quad (8)$$

where n is the complex refractive index, η the real part of the refractive index, and κ the imaginary part, also referred to as the extinction coefficient.

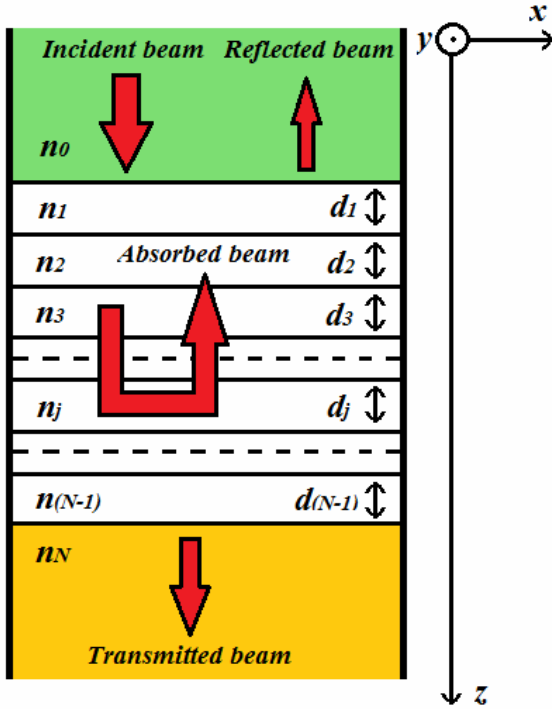


Figure 3. Multilayer optical structure

$E(z)$ and $H(z)$ are the complex amplitudes of the electric and the magnetic fields respectively, that are the solutions of Maxwell's equations in a plane $z = \text{constant}$.

It is known that across a surface discontinuity of ϵ and μ , the tangential components of the electric and magnetic fields are continuous. Hence, at normal incidence, the relation between their

amplitudes at the entrance and the exit of a layer is given by Eqs. 9-13,

$$[A(z)] = [M_j(\sigma)] [A(z+d)] \quad (9)$$

$$[A(z)] = \begin{bmatrix} E(z) \\ H(z) \end{bmatrix} \quad (10)$$

$$[M_j(\sigma)] = \begin{bmatrix} \cos \beta_j & \frac{i}{g_j} \sin \beta_j \\ i g_j \sin \beta_j & \cos \beta_j \end{bmatrix} \quad (11)$$

$$\beta_j = 2\pi \cdot \sigma \cdot n_j(\sigma) \cdot d_j \quad (12)$$

$$g_j = n_j(\sigma) \cdot \sqrt{\frac{\epsilon_0}{\mu_0}} \quad (13)$$

M_j is called the characteristic matrix of a layer j depending on the wave number σ .

The result may be generalized to the case of a system Σ composed of a superposition of $N-1$ layers, its characteristic matrix M_Σ is obtained by the classical rules of matrix multiplication, as shown by Eq. 14.

$$[M_\Sigma(\sigma)] = [M_1(\sigma)] \cdot [M_2(\sigma)] \cdot \dots \cdot [M_{N-1}(\sigma)] \quad (14)$$

We wish to emphasize that the order of the product factors is important, as matrix multiplication is non-commutative. Indeed, there is no reason for the system to be insensitive to the order of its constituents.

Moreover, this formalism is particularly convenient to model the refractive index gradient between two layers such as the substrate and the active zone. One only has to describe it as a multitude of thin layers with a gradual variation of indices, thus allowing a smooth transition.

The structure characteristic matrix is then used to calculate the reflected, transmitted and absorbed flux named $R(\sigma)$, $T(\sigma)$ and $A(\sigma)$ respectively, using Eqs. 15-19, where N refers to the exit medium properties.

$$\begin{bmatrix} B(\sigma) \\ C(\sigma) \end{bmatrix} = [M_\Sigma(\sigma)] \cdot \begin{bmatrix} 1 \\ g_N(\sigma) \end{bmatrix} \quad (15)$$

$$g_\Sigma(\sigma) = \frac{C(\sigma)}{B(\sigma)} \quad (16)$$

$$R(\sigma) = \left| \frac{g_0(\sigma) - g_\Sigma(\sigma)}{g_0(\sigma) + g_\Sigma(\sigma)} \right|^2 \quad (17)$$

$$T(\sigma) = [1 - R(\sigma)] \cdot \frac{\Re[g_N(\sigma)]}{\Re[B(\sigma) \cdot C(\sigma)]} \quad (18)$$

$$A(\sigma) = 1 - [R(\sigma) + T(\sigma)] \quad (19)$$

$g_\Sigma(\sigma)$ could be considered as the effective refractive index of the structure Σ .

In the case of Microspoc, a characteristic matrix is associated to each pixel. The structure is composed of a substrate of CdZnTe, an active layer HgCdTe, and a metal layer at the bottom, represented by the matrices M_s , M_{ah} , and M_m respectively.

Thus, the characteristic matrix of each elementary detector is given by Eq. 20.

$$[M_{Microspoc}(\sigma)] = [M_s(\sigma)] \cdot [M_{ah}(\sigma)] \cdot [M_m(\sigma)] \quad (20)$$

We suppose that the totality of the electron-hole pairs generated by the absorbed photons is collected. Therefore, the quantum efficiency of the pixel is represented by the absorption coefficient $A(\sigma)$.

There is a high number of parameters in this model and some of them are impossible to estimate precisely, due to an important lack of knowledge on the optical properties and the technological process. Thus, we developed an analytical model with fewer parameters to extract. Ideally, this model should fit as much as possible the physical model.

2.3. Analytical model

As explained above, there are actually several waves interfering in the structure, making the Fourier transform inadequate to extract the scene spectrum. It can be shown [4] that a first good approximation is to consider the three major waves interfering.

Under some simplifying hypothesis [4], the detector efficiency can then be described by Eq. 21,

$$\begin{aligned} \eta(\sigma, x) = & \eta_0(\sigma, x) \\ & + \Phi(\sigma, x) \cdot \cos[2\pi \cdot \sigma \cdot \delta_s(\sigma, x)] \\ & + \Omega(\sigma, x) \cdot \cos[2\pi \cdot \sigma \cdot (\delta_s(\sigma, x) + \delta_{al}(\sigma, x))] \\ & + \Psi(\sigma, x) \cdot \cos[2\pi \cdot \sigma \cdot \delta_{al}(\sigma, x)] \end{aligned} \quad (21)$$

where σ is the wave number, x is the pixel

coordinate, η_0 its mean quantum efficiency, Φ , Ω , Ψ the modulation amplitudes, δ_s and δ_{al} are respectively the substrate and the active layer optical path differences.

One must notice that for high wave numbers, Ω and Ψ become negligible with respect to Φ , which represents the two-wave regime plotted on Fig. 2.

The next step will now consist in estimating the scene spectrum from a bi-dimensional interferogram, by performing robust inversion of this model.

Previous results were published [14,15], using a purely measured matrix M . Even if they contained parasitic oscillations, they are promising, and we wish to obtain better results thanks to our modeling approach.

3. CONCLUSION

A modeling approach was proposed for an infrared stationary Fourier transform spectrometer. The compact detector structure was described. We presented a physical model and an analytical one that will be used in order to perform a robust inversion of interferograms. The physical model is based on a multilayer description using indices and thicknesses of the different layers under normal incidence assumption, whereas the analytical model is a simpler description of the interference phenomena involving only the three major waves.

Several techniques of inversion will be tested using these models, such as truncated singular value decomposition [15] or quadratic regularization. Moreover, other processing methodologies will be investigated in order to access to robust spectra that satisfy the expected specifications. The results will enhance the resources to meet new instrumentation challenges.

4. REFERENCES

1. Guérineau, N., Suffis, S., Cymbalista, P. & Primot, J. (2004). Conception of a stationary Fourier transform infrared spectroradiometer for field measurements of radiance and emissivity. *SPIE*. **5249**, 441-448.
2. Voge, P., & Primot, J. (1998) Simple infrared Fourier transform spectrometer adapted to low light level and high-speed operation. *Optical Engineering*. **37**, 2459-2466.
3. Rommeluère, S., Guérineau, N., Deschamps, J., De Borniol, E., Million, A., Chamonal, J.P. & Destefanis, G. (2004). Microspectrometer on a chip (MICROSPOC) : first demonstration on a 320x240

LWIR HgCdTe focal plane array. *SPIE*. **5406**, 170-177.

4. Rommeluère, S., (2007). Intégration d'un microspectromètre statique par transformée de Fourier sur un plan focal infrarouge, PhD thesis, Université Paris-Sud.

5. Barnes, T. H. (1985). Photodiode array Fourier transform spectrometer with improved dynamic range. *Applied Optics*, **24**(22), 3702-3706.

6. Junttila, M. L., Kauppinen, J., & Ikonen, E. (1991). Performance limits of stationary Fourier spectrometers. *JOSA A*, **8**(9), 1457-1462.

7. Junttila, M. L. (1992). Stationary Fourier-transform spectrometer. *Applied Optics*, **31**(21), 4106-4112.

8. Guérineau, N., Rommeluère, S., Gillard, F., Ferrec, Y., Henry, D., Primot, J., Deschamps, J., Taboury, J. & Fendler, M. (2010). Recent developments in stationary Fourier transform spectrometry for field measurements of infrared signatures. In Optro2010 International Symposium on Optronics in Defence and Security.

9. Benoît-Pasanau, C., Gillard, F., Ferrec, Y., Lefebvre, S., Rommeluère, S., Guérineau, N. & Primot, J. (2012). Relevance of an inverse problem approach to overcome cut-off wavenumbers disparities in infrared stationary Fourier transform spectrometers. *Applied Optics*. **51**, 1660-1670.

10. Rommeluère, S., Guérineau, N., Haidar, R. Deschamps, J., De Borniol, É., Million, A., Chamonal, J.-P. & Destefanis, G. (2008). Infrared focal plane array with a built-in stationary Fourier-transform spectrometer: basic concepts. *Optics Letters*. **33**, 1062-1064.

11. Rommeluère, S., Haidar, R., Guérineau, N. Deschamps, J., De Borniol, É., Million, A., Chamonal, J.-P. & Destefanis, G. (2007). Single-scan extraction of two-dimensional parameters of infrared focal plane arrays utilizing a Fourier-transform spectrometer. *Applied Optics*. **46**, 1379-1384.

12. van Heel, A. C. S. (1967). *Advanced optical techniques*. Advanced Optical Techniques by ACS Van Heel New York, NY: John Wiley and Sons, INC. **1**.

13. Macleod, H. A. (2001). *Thin-film optical filters*. CRC Press.

14. Ferrec, Y., Rommeluère, S., Lefebvre, S., Benoît, C., Gillard, F., & Guérineau, N. (2011). Infrared focal plane array with a built-in stationary Fourier-transform spectrometer (MICROSPOC): physical limitations and numerical solutions. In

'Fourier Transform Spectroscopy'. *Optical Society of America*.

15. Gillard, F., Lefebvre, S., Ferrec, Y., Mugnier, L., Rommeluère, S., Benoit, C. & Taboury, J. A. (2011). Inverse problem approaches for stationary Fourier transform spectrometers. *Optics letters*. **36**(13), 2444-2446.



BP 72 - 29 avenue de la Division Leclerc - 92322 CHATILLON CEDEX - Tél. : +33 1 46 73 40 40 - Fax : +33 1 46 73 41 41

www.onera.fr